JCTC Journal of Chemical Theory and Computation

Molecular Dynamics Study of a Surfactant Monolayer Adsorbed at the Air/Water Interface

Jnanojjal Chanda and Sanjoy Bandyopadhyay*

Molecular Modeling Laboratory, Department of Chemistry, Indian Institute of Technology, Kharagpur - 721302, India

Received February 3, 2005

Abstract: A constant volume and temperature (NVT) molecular dynamics (MD) simulation has been carried out to investigate the properties of a monolayer of monododecyl hexaethylene glycol ($C_{12}E_6$) adsorbed at the air/water interface at a surface coverage corresponding to that at its critical micelle concentration (55 Å^2 per molecule). The simulated results have been found to agree reasonably well with available experimental data and with other simulation studies. The study shows that the long polar headgroups of the surfactants are more tilted toward the aqueous layer due to strong interaction between them and water. It has been shown that the surfactant monolayer strongly influences the translational and rotational mobility of interfacial water molecules. A drastic change in the dipolar reorientational motion of water molecules in the aqueous layer is observed with a small variation of distance from the surfactant headgroups.

1. Introduction

The study of the structure and dynamics of organized surfactant assemblies at different interfaces and in bulk solutions is of great importance in various industrial processes, such as detergency, oil recovery, purification, food processing, paints, lubrication, and so forth.[1] Much successful work has been done to understand the properties of surfactant aggregates in solutions,[2−4] but at interfaces, proper systematic studies of adsorbed films are still lacking. This is mainly due to the general lack of suitable experimental techniques capable of probing wet interfaces.

In this work we have focused on the surfactant $C_{12}E_6$, which is a member of an important group of nonionic surfactants, known as the C_mE_n family. These are monoalkyl ethers of the form $C_mH_{2m+1}(OC_2H_4)_nOH$, with a long headgroup consisting of a hydroxy (OH) group followed by a variable number of polar OC_2H_4 (E) groups and a nonpolar C_mH_{2m+1} tail, also of variable length. Polyoxyethylene surfactants (which share the E_n headgroup but may have more complicated hydrophobic tail structures) are the most important nonionic surfactants in commercial use.[1] In particular, the C_mE_n family of surfactants are used in the detergency, cosmetics, and pharmaceutical industries. These surfactants are also highly important from a theoretical point of view, since systematic variation of the values of *m* and *n* alters the properties of the surfactant toward hydrophobicity or hydrophilicity and thus can provide valuable insight into the mechanisms governing self-assembly phenomena in these systems.

A large number of experimental studies have been reported on the properties of different surfactant layers adsorbed at vapor/liquid, liquid/liquid, and liquid/solid interfaces. Richmond and co-workers[5] have studied the structure and orientation of interfacial water molecules using vibrational sum frequency spectroscopy on both cationic and anionic surfactant monolayers at the air/water interface. They have also studied in detail the conformational order of different surfactant monolayers adsorbed at the water/carbon tetrachloride (CCl_4) interface at different surface coverages.[6,7] Grubb et al.[8] have compared the orientation of surfactant molecules at air/water, water/decane, and water/CCl_4 interfaces using second harmonic generation studies. Recently, time-resolved quasielastic laser scattering measurement has been applied to study the dynamics and collective properties of anionic surfactant sodium dodecyl sulfate (SDS) and neutral surfactant Triton X-100 adsorbed at water/nitrobenzene interface.[9] Fluorescence[10] and resonance Raman spec-

* Corresponding author phone: 91-3222-283344; fax: 91-3222-255303; e-mail: sanjoy@chem.iitkgp.ernet.in.

10.1021/ct050019y CCC: $30.25
Published on Web 07/15/2005

tra[11] have also been used in earlier studies on different surfactant monolayers adsorbed at liquid/liquid interfaces. Recently, Linse and co-workers[12] have studied adsorption of several nonionic surfactants at liquid/vapor and solid/liquid interfaces using surface tension and ellipsometric measurements. Only recently, the relatively new technique of neutron reflection has been successfully employed by Thomas and co-workers[13−17] to study the properties of various surfactant layers, including C_mE_n type of surfactants adsorbed at air/liquid, liquid/liquid, and liquid/solid interfaces. Neutron experiments are capable of providing accurate information on the density profiles of the surfactant at an interface. Neutron reflection measurements with isotopic substitution can provide information on structural characteristics of different fragments of the molecules comprising the monolayer.[13,14] Thomas and co-workers[13,14] have studied in detail the adsorption of a series of monododecyl ether surfactants, $C_{12}E_n$, at the air/water interface by varying the number of oxyethylene headgroups between $n = 1$ to $n = 12$. The structure of adsorbed layers were determined by increasing the concentration of the surfactants from a low value to the critical micelle concentration (cmc). It is observed that the alkyl chain thickness remained constant throughout the series, and the value of structural parameters indicate a large average tilt of the surfactant molecules away from the surface normal. These experiments also indicate that the surfactant layers are roughened at the interface with significant intermixing of alkyl chains and oxyethylene headgroups.

The time scales associated with the adsorption of surfactants leading to the formation of a monolayer at the air/water interface or the exchange of monomers between the monolayer and those in the bulk solution are in the range of micro- to milliseconds and therefore are beyond the scope of current generation atomistic molecular dynamics (MD) simulations. However, it is possible to study the microscopic properties of a monolayer already adsorbed at an interface within a reasonable time. This approach has been employed in several simulation studies.[18−32] Tarek et al.[18] have carried out MD studies of cationic surfactant cetyltrimethylammonium bromide (CTAB) adsorbed at the air/water interface at two different concentrations. The simulated density profiles were found to be in good agreement with neutron reflectivity data. Wijmans and Linse[22] have used the Monte Carlo method to study the self-assembly of nonionic surfactants at a hydrophilic surface. Berkowitz and co-workers[19,23,24] have studied in detail the monolayers of ionic surfactants adsorbed at air/water and water/CCl_4 interfaces. They observed a significant difference in the molecular configuration of the surfactants adsorbed at the two interfaces.[19] It was also shown that the polarity of a surfactant has strong influence on the structure and dynamics of water near the interface.[23] Kuhn and Rehage[25−27] have studied in detail the orientation and dynamic properties of monododecyl pentaethylene glycol ($C_{12}E_5$) monolayer adsorbed at air/water and oil/water interfaces. Recently, Rossky and co-workers[28,29] have reported atomistic MD simulation studies on fluorocarbon surfactant monolayers at CO_2/water interface. They noticed that water penetrated the fluorocarbon surfactants to a lesser extent compared to the hydrocarbon surfactants. We have recently studied monolayers of monododecyl diethylene glycol ($C_{12}E_2$) as well as AOT adsorbed at the air/water interface using atomistic MD simulations.[20,21] Only recently, Smit and co-workers[30,31] have used the dissipative particle dynamics method to study the properties of surfactant monolayers at an oil/water interface. They have investigated the effect of the surfactant structure on the bending moduli of the adsorbed monolayers. MD simulations of monolayers of anionic−nonionic surfactant mixtures at a liquid/liquid interface has also been reported recently.[32]

In this work, the microscopic properties of monolayers of monododecyl hexaethylene glycol, $C_{12}E_6$, adsorbed at the air/water interface at a surface coverage corresponding to its cmc (55 Å^2 per molecule) have been studied using MD simulation techniques. The structure and dynamics of the adsorbed monolayer films as well as that of the interfacial water molecules have been investigated in detail at an atomic level resolution. We have organized the article as follows. In the next section we discuss the setup of the system, and the simulation methods employed. This is followed by the results obtained from our investigations and their interpretation. In the last section we summarize the important findings obtained from our study.

2. System Setup and Simulation Details

To study a surfactant monolayer adsorbed at an interface, one has to carefully handle the long-range electrostatic interactions along with a proper choice of boundary conditions. In accordance with our earlier studies,[20,21] we set up the system by placing two monolayers on opposite sides of a slab of aqueous solution, which is thick enough for the two monolayers to remain effectively isolated from each other.

The initial configuration of our constant temperature and volume (NVT) simulation system was set up by arranging a uniform monolayer of 64 surfactants with their hydroxy groups on an appropriate 8×8 square lattice in the *xy* plane with the hydrocarbon chains directed perpendicular to the lattice plane in extended configurations. The lattice constants were chosen to give the surface area per molecule of 55 Å^2, corresponding to the experimentally observed value for adsorption at the air/water interface at cmc.[33] Then two such Langmuir type monolayers were placed, with their hydroxy groups solvated, in the *xy* plane of a roughly 35 Å thick slab of water molecules. The thickness of the aqueous layer was large enough to give a distinct region of bulk solution in the middle of the simulation cell. The overall system contained 128 surfactants and 4133 water molecules. The dimension of the simulation cell in the *x* and *y* directions was 59.4 Å, while the *z* dimension was kept large at ∼200 Å. It is assumed that such large *z* dimension results in negligible interactions between periodic replicas in the *z*-direction.

Initially the surfactant headgroups and the water molecules were kept frozen and a short MD run of 10 ps was performed at a high temperature of 1000 K. This is done to randomize the conformations of the hydrocarbon chains of the surfactants. The surfactant headgroups and the water molecules were then unfrozen, and the temperature of the system was

lowered to 10 K. The temperature was then slowly increased to 298 K over next 50 ps. The resulting configuration was then equilibrated at constant temperature ($T = 298$ K) and volume (NVT) for about 2 ns. This was followed by a production run of another 3.5 ns duration. The trajectories were stored during the production phase of the simulation for subsequent analysis.

The simulations utilized the Nosé-Hoover chain thermostat extended system method[34] as implemented in the PINY-MD simulation code.[35] A recently developed reversible multiple time step algorithm, RESPA,[34] allowed us to employ a 4 fs MD time step. This was achieved using a three-stage force decomposition into intramolecular forces (torsion/bend-bond), short-range intermolecular forces (a 7.0 Å RESPA cutoff distance), and long-range intermolecular forces. Electrostatic interactions were calculated by using the particle mesh Ewald (PME) method.[36] The PME and RESPA were combined following the method suggested by Procacci et al.[37,38] The minimum image convention[39] was employed to calculate the Lennard-Jones interactions and the real-space part of the Ewald sum using a spherical truncation of 7 and 10 Å, respectively, for the short- and the long-range parts of the RESPA decomposition. 'SHAKE/ROLL' and 'RATTLE/ROLL' methods[34] were implemented to constrain all bonds involving hydrogen atoms to their equilibrium values.

The intermolecular potential model was based on pairwise additive site−site electrostatic and Lennard-Jones contributions. The rigid three-site SPC/E model[40] was employed for water. The CH_3 and CH_2 groups of the surfactants were treated as united atoms (i.e. these groups were represented by single interaction sites). The potential parameters for the alkane chain groups were taken from the work of Martin and Siepmann,[41] while the oxyethylene groups were modeled using the OPLS parameters.[42,43] The surfactant chains were made flexible by including bond stretching, bending, and torsion interactions.

3. Results and Discussion

3.1. Structural Properties. The configurations of the system at the beginning (a) and at the end of the simulation (b) are displayed in Figure 1. It is clear from the figure that the monolayer lost its initial ordering during the nanosecond time scale of the simulation. The important notable feature from the figure is that, as the simulation progressed, a significant roughness developed near the surfactant headgroup region of the interface. This is in contrast to an almost flat interface at the beginning. The structural properties of the monolayers can be obtained by studying various distribution functions. In Figure 2(a) we display the average number density profiles (NDP) of different components of the surfactant chains from the center of the simulation cell in a direction normal to the plane of the interface (z). The different components of the surfactants for which the NDPs are computed separately include the terminal hydroxy group (OH), the oxyethylene groups (E), and the hydrocarbon chain atoms (C). The distribution for the water molecules is also computed and plotted. The primary features of the plot are similar to the well-known picture of the surfactant organization at an interface.[18−21,32,44] The surfactant headgroups are hydrated and reside at the interface, while the hydrocarbon tails are excluded from water. Only a fraction of water penetrated within the hydrocarbon tail part of the surfactants. Distribution of a few selected oxyethylene groups (E1, E3, and E6) as displayed in Figure 2(b) shows clearly that almost the entire oxyethylene headgroup region is hydrated. This suggests that the polar nature of the long oxyethylene headgroups helps water molecules penetrate the monolayer film. Finally, the symmetric nature of the density profiles of the two monolayers indicates a well-equilibrated system with an identical overall structure of the two monolayers. The presence of an approximately 25 Å thick slab of bulk water between the two layers indicates that they are independent and have no influence on each other. Further insight into the structure of the surfactant monolayers was obtained from the probability distribution function of the oxyethylene groups (E1−E6) of the surfactants with respect to the normal (z) to the plane of the interface. This is shown in Figure 3 separately for the two monolayers. Again with regard to their average structure the two monolayers are very similar. The relatively broader distributions of the first two oxyethylene groups (E1 and E2) indicate the roughness of the monolayer structure at the interface.

We have calculated the thickness of the adsorbed monolayers from the simulated MD trajectory. The time evolution of the overall thickness (d_s) averaged over both the monolayers is shown in Figure 4. The figure also displays separately the time evolution of the thickness of the oxyethylene (E1−E6) headgroup part (d_h) and the dodecyl hydrocarbon chain (d_t). The presence of sharp oscillations in the plots again indicates the roughness of the adsorbed monolayers. The average thickness values as obtained from our calculations are listed in Table 1. For comparison, the corresponding values obtained from neutron reflection studies[14,33] are also listed in the table. Considering the approximations involved in the models used to obtain the area per molecule and the widths of the profiles from neutron reflectivity measurements, our results agree reasonably well with the experimental data. The accuracy of the force field employed might also be responsible to some extent for the deviations noticed, particularly for the thickness of the hydrophilic headgroup moiety. However, the most interesting feature to note from this result is that the sum of the thicknesses of the two constituent parts of the surfactant molecule is greater than its overall thickness. This suggests that there is an extensive mixing of the head and tail parts of the surfactant chains. The extent of such mixing is in accordance with the density distribution as shown in Figure 2. There appears to be no distinction between the two parts of the surfactants in the adsorbed layer. A similar behavior was observed recently for surfactants with much smaller headgroups ($C_{12}E_2$) adsorbed at an interface.[20]

3.2. Surfactant Orientations. To investigate the orientation of head and tail parts of the surfactants at the interface, we have calculated the orientation of the head and the hydrocarbon tail vectors with respect to the normal (z) to the plane of the interface. The head vector is defined as the vector connecting the hydroxy group and the oxygen atom

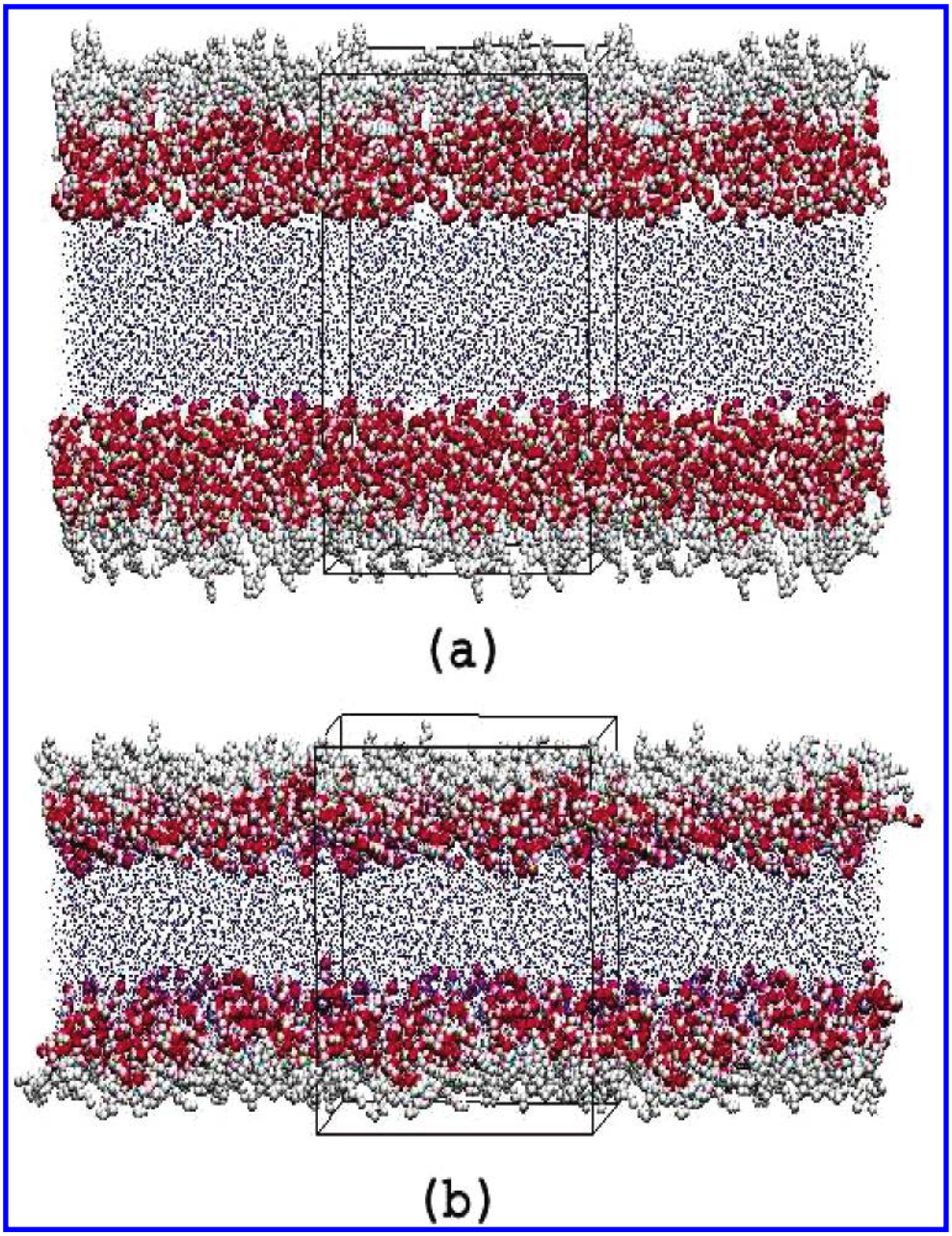

Figure 1. Snapshots of the configuration of the system near the beginning (a) and at the end (b) of the simulation. The oxygen atoms, methyl (CH_3), and methylene (CH_2) groups of the surfactant molecules are drawn as spheres, while only the oxygen atoms of the water molecules are drawn as dots. The atom coloring scheme is O (surfactant), red; CH_3/CH_2, gray; and O (water), blue. For visual clarity, the system is replicated once on both sides of the central simulation cell and the dimension of the cell is marked arbitrarily in the direction normal to the plane of the interface (i.e., along the *z* direction).

of the last oxyethylene group (E6). The vector that connects the first methylene group (CH_2) and the terminal methyl group (CH_3) of the dodecyl chain is defined as the tail vector. The probability distribution, $\rho(\theta)$, of the tilt angle (θ) between the head or tail vector with respect to the normal to the interface (z) is displayed in Figure 5. The distributions are calculated by taking an average over both the monolayers. It is clear from the figure that both the head and tail parts of the surfactant molecules are significantly tilted from the normal (z). The average tilt angle values of the head and tail vectors have been found to be 56.8° and 54°, respectively. This average value of the tilt angle of the dodecyl hydrocarbon chain is comparable with the reported experimental value of 45°.[14] However, the most noticeable feature of the distribution is the presence of a significant fraction (∼13%) of the head vectors oriented with an angle of $\theta \geq 90°$. This suggests that some of the head vectors are reoriented at the interface. Such a reorientation occurs because of a strong interaction between the water molecules and the polar oxyethylene headgroups of the surfactants. Similar orientational bahavior was observed recently with adsorbed $C_{12}E_2$ surfactant monolayers.[20]

3.3. Surfactant and Water Dynamics. To obtain further insight into the microscopic properties of the adsorbed surfactant monolayer, it is crucial to investigate the dynamics of the surfactant molecules as well as the water around them.

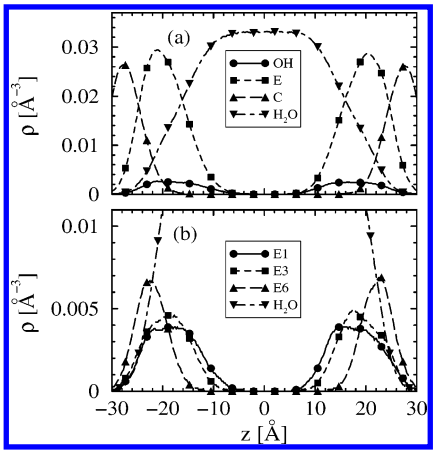

Figure 2. (a) Number density profiles of the hydroxy group (OH), oxyethylene groups (E), hydrocarbon chain atoms (C), and water molecules, measured with respect to the center of the simulation cell in the direction normal to the plane of the interface (i.e., along the *z* direction). The density profiles of a few selected oxyethylene groups are shown in (b). The oxyethylene E groups are numbered starting from the terminal OH group of the surfactant molecule.

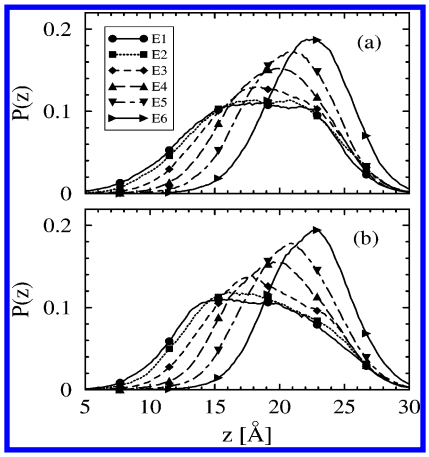

Figure 3. The distribution of the individual oxyethylene groups (E1−E6) of the surfactant molecules along the *z*-direction. The distributions for the two layers are drawn separately in (a) and (b). The numbering scheme of the E groups is the same as in Figure 2.

The dynamical behavior of the surfactants and water molecules are discussed in this section.

3.3.1. Surfactant Dynamics. The translational mobility of the surfactant molecules can be investigated by measuring the mean square displacements (MSD) of the center of mass of the surfactant chains from the MD trajectory. To investigate whether the adsorbed surfactant molecules exhibit any anisotropy in their translational mobility, we have separately measured the center of mass MSDs in the plane of the interface (i.e., *xy* plane) and in the direction normal to it (i.e., along the *z* direction). These are displayed in Figure 6. We notice from the figure that the in-plane motion of the surfactant molecules is higher than the out-of-plane motion. Slightly higher in-plane mobility arises from the lateral rattling motion of the surfactant molecules, which dominates the time scale over which the calculations are carried out.

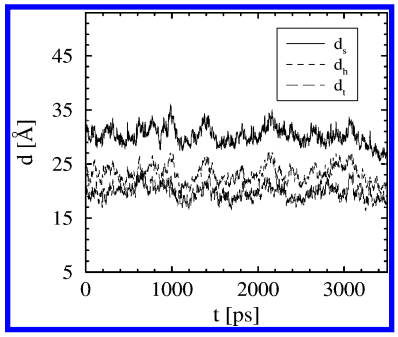

Figure 4. Time evolution of the thickness of the monolayer during the last 3.5 ns of the simulation. The thickness of the whole surfactant chain (d_s) is drawn as a solid line, while that of the oxyethylene headgroups (d_h) and the hydrocarbon tail (d_t) are drawn as broken lines. The calculation is done by averaging over both the monolayers.

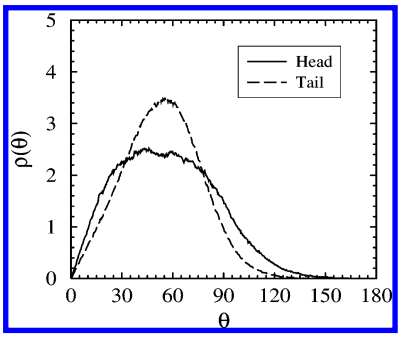

Figure 5. Distribution of the tilt angle, θ (in degrees), of the oxyethylene headgroup (solid line) and the hydrocarbon tail (dashed line) with respect to the normal to the interface, *z*.

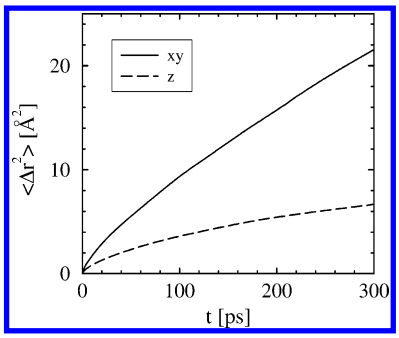

Figure 6. Time evolution of the in-plane (i.e., in *xy* plane) and the out-of-plane (i.e., along *z*) mean square displacements of the center of mass of the surfactant molecules.

Table 1: Comparison of MD and Experimental Values[14,33] of the Oxyethylene Group Thickness (d_h), Dodecyl Chain Thickness (d_t), and the Overall Thickness (d_s) of $C_{12}E_6$ Monolayers Adsorbed at the Air/Water Interface at a Surface Coverage of 55 Å^2 Per Molecule

quantity (Å)	MD	experiment
d_h	23.2 ± 1.0	19.5 ± 1.0
d_t	19.7 ± 0.9	19.0 ± 1.0
d_s	30.3 ± 1.3	26.5 ± 2.0

The out-of-plane protrusion motion of the surfactants is more restricted. Such restricted dynamics of the surfactant molecules is a signature of anomalous sublinear diffusion in heterogeneous anisotropic or confined systems.[45,46] To

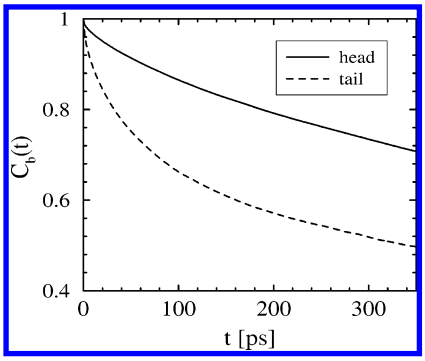

Figure 7. Reorientational time autocorrelation functions for the oxyethylene head vectors and the hydrocarbon tail vectors of the surfactant molecules.

investigate the extent of anomalous diffusion, if any, the curves in Figure 6 are fitted to a law

$$\langle \Delta r^2 \rangle \simeq t^{\alpha} \tag{1}$$

where the exponent α is expected to be smaller than one. The estimated values of α have been found to be 0.53 and 0.32 for the in-plane and out-of-plane motions, respectively. Such small α values clearly show the presence of significant anomaly in the diffusion behavior of surfactant molecules within the time scale of our simulation.

The rotational motion of the surfactant molecules has been investigated by measuring the reorientational dynamics of the head and tail vectors (as defined earlier) of the individual monomers. The reorientational motion has been studied by measuring the time correlation function (TCF), $C_b(t)$, defined as

$$C_b(t) = \frac{\langle \hat{b}_i(t+\tau).\hat{b}_i(\tau)\rangle}{\langle \hat{b}_i(\tau).\hat{b}_i(\tau)\rangle} \tag{2}$$

where $\hat{b}_i(t)$ represents the unit vector corresponding to the head or tail of the *i*th surfactant molecule at time *t*, and the angular brackets denote averaging over the surfactant molecules and over initial times τ. The variation of $C_b(t)$ against time has been displayed in Figure 7. It is clearly evident from the figure that the headgroups of the surfactant molecules reorient much slowly than the hydrocarbon tails. Such slow relaxation of $C_b(t)$ for the headgroups arises from the strong interaction between the interfacial water molecules and the oxyethylene groups, as mentioned before. The hydrocarbon tails of the surfactants being away from the interface are more flexible in nature and thus reorient faster.

3.3.2. Water Dynamics. The dynamics of water near the interface plays a crucial role in determining the behavior of surfactant aggregates. The water dynamics near the surface of organized molecular assemblies such as micelles[47−49] and heterogeneous macromolecules such as proteins[50] is well studied. However, the dynamics of water near the surface of an adsorbed surfactant film has not been explored much. In this section we study the translational and reorientational motion of water near the interface.

3.3.3. Translational Motion of the Interfacial Water. The mean square displacements of water molecules at different distances from the interface have been calculated. To be

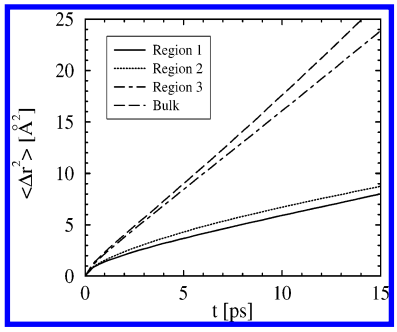

Figure 8. Mean square displacement (MSD) of the water molecules in different regions of the aqueous layer. Region 1 comprises water molecules which are within 4 Å from the hydroxy group oxygen atoms, those which are within 4−7 Å are in region 2, while those which are beyond 7 Å are said to be in region 3. The MSD of water molecules in pure bulk water is also shown for comparison.

Table 2: Diffusion Coefficient of the Water Molecules in Different Regions as Obtained from Their Mean Square Displacements[a]

region	D (10^{-5} cm^2 s^{-1})
region 1 (0−4 Å)	0.72
region 2 (4−7 Å)	0.73
region 3 (>7 Å)	2.57
bulk water	2.84

[a] The value for bulk water is also listed for comparison.

specific, we have defined three hydration regions. Water molecules which are within a distance of 4 Å from the hydroxy group oxygen atoms of the surfactant headgroups form region 1. This essentially corresponds to the first hydration layer with respect to the hydroxy group oxygen atoms of the surfactants. Region 2 comprises water molecules within 4−7 Å from the hydroxy group oxygen atoms, while those beyond 7 Å are considered to be in region 3. The distances are measured with respect to both the monolayers by tagging the water molecules at different time origins. The plots are displayed in Figure 8. For comparison, we have also displayed the same for pure bulk water, which was obtained from a MD simulation of pure SPC/E water at room temperature. It is evident from the figure that at a distance close to the surfactant headgroups (region 1) the translational mobility of the water molecules is significantly restricted. The mobility of water molecules increases as the distance from the surfactant headgroups is increased. Within a short distance of approximately 7 Å from the interface (region 3), the mobility of the water molecules approaches close to that of pure bulk water. Such restricted mobility of water near the interface of organized molecular assemblies, such as micelles as well as surfactant aggregates at an interface, has been studies recently.[21,47−49] This might arise because of the strong interaction between the hydrophilic oxyethylene headgroups of the surfactants and the surrounding water molecules. The diffusion coefficients of water molecules in the three regions have been calculated from a linear fit to the corresponding mean square displacements, which are listed in Table 2. The data show that water in regions 1 and 2 are much less mobile than those in region 3 and pure bulk water. In fact, the water in region 3 exhibits three times faster

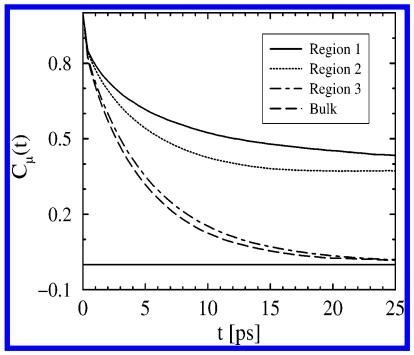

Figure 9. Reorientational time correlation function (TCF) of the water dipoles, $C_\mu(t)$, for the water molecules in three regions of the aqueous layer. The definitions of the regions are same as in Figure 8. The TCF for pure bulk water is also shown for comparison.

dynamics than those in region 1. Such an approach to calculate the diffusion coefficients of interfacial water molecules from MD simulations has been used earlier.[21,49] It may be noted that the absolute values of the calculated diffusion coefficients may not be very authentic in this case. This is because the surfactant monolayers provide a heterogeneous anisotropic environment for the water molecules, which is not strictly three-dimensional.[45,46] However, here we are more interested in comparing the relative diffusion of water in different regions close to the interface, rather than measuring the absolute diffusion coefficient values.

3.3.4. Orientational Motion of the Interfacial Water. It is expected that the rotational motion of the water molecules close to the surfactants at the interface will also be affected. The rotational motion of water can be investigated by measuring the reorientational dynamics of its electrical dipole $\vec{\mu}$, defined as the vector connecting the oxygen atom of the water molecule to the center of the line connecting the two hydrogen atoms. The time evolution of $\vec{\mu}$ can be estimated by measuring the dipole−dipole time correlation function (TCF), defined as

$$C_\mu(t) = \frac{\langle \hat{\mu}_i(t+\tau).\hat{\mu}_i(\tau)\rangle}{\langle \hat{\mu}_i(\tau).\hat{\mu}_i(\tau)\rangle} \qquad (3)$$

where $\hat{\mu}_i(t)$ is the unit dipole moment vector of the ith water molecule at a time t, and the angular brackets denote averaging over the tagged water molecules and over initial times τ. Again, we restrict ourselves to the reorientational motion of water molecules in the three regions as discussed before. The correlation functions were calculated by averaging over these water molecules only, which are shown in Figure 9. For comparison, the decay curve for pure bulk water is also displayed. It is clear from the figure that the relaxation curves decay nonexponentially, and for water close to the surfactants (regions 1 and 2) they do not decay to zero. This shows that the presence of the surfactants significantly restricts the reorientational motion of water. However, similar to translational mobility, the rotational motion of the water molecules too approach that of pure bulk water within a short distance of about 7 Å (region 3). The slowing down of the rotational dynamics of interfacial water has been shown recently in an adsorbed monolayer of anionic surfactants, AOT.[21] Thus the present investigation in conjunction with our earlier work establishes the fact that the restricted dynamics of the interfacial water in an adsorbed surfactant monolayer is independent of the type of the surfactant molecules. To obtain a quantitative estimation of the time scales associated with the reorientational motion of the water molecules from the dipolar correlation functions, we have fitted the correlation functions with multiexponentials. It is a common practice to use multiexponentials, as one can then directly obtain time constants associated with different motions.[21,47] These time constants can be assigned to different relaxation processes of the system. Here we have used a sum of three exponentials to fit the data for each of the three TCFs. The parameters for best fit are shown in Table 3. The average reorientational time constant ($\langle\tau_\mu\rangle$) values clearly indicate that the rotational motion of water close to the surfactant headgroups is severely restricted. The slow decay for water close to the interface arises because of their strong interaction and formation of hydrogen bonds with the polar oxyethylene headgroups of the surfactants. As the dynamics of the individual surfactant chains in the adsorbed monolayer is much slower compared to the time scale of water dynamics, such strong surfactant−water interaction slows down the reorientational motion of these water molecules *bound* to the interface. Interestingly, an extraordinary slow decay with a long time component (nearly flat decay curve), which we could not determine because of the limitation of the time scale of our simulation has been observed for water molecules in region 2. It has been found that the unusually slow decay for water in region 2 arises due to the presence of a small fraction of water molecules which are pulled into the monolayer by the long polar oxyethylene headgroups and remain trapped for long times. It may be noted that the $\langle\tau_\mu\rangle$ value for water in region 3 approaches that for pure bulk water and is about 13 times smaller than that for water in region 1. Such drastic changes in the reorientational motion of water molecules with a slight variation of distance from the surfactant headgroups of an adsorbed monolayer has also been observed recently.[21]

Table 3: Multiexponential Fitting Parameters for the Dipolar Time Correlation Functions of Water Molecules in Different Regions[a]

region	time constant (ps)	amplitude (%)	$\langle\tau_\mu\rangle$ (ps)
region 1 (0−4 Å)	0.24	14.5	66.13
	4.57	32.7	
	122.26	52.8	
region 2 (4−7 Å)	0.19	13.0	-
	4.73	50.5	
	>500	36.5	
region 3 (>7 Å)	0.18	12.5	5.12
	4.29	54.4	
	8.38	33.1	
bulk water	0.22	13.8	4.73
	4.68	80.6	
	16.63	5.6	

[a] $\langle\tau_\mu\rangle$ is the average time constant. Corresponding parameters for bulk water are also listed for comparison.

4. Conclusion

In this article, we have presented results obtained from an atomistic MD simulation study of the structure and dynamical properties of adsorbed monolayers of the nonionic surfactant $C_{12}E_6$ adsorbed at the air/water interface. The simulation has been performed at a constant volume and at room temperature with a surface coverage of 55 Å^2 per molecule, which corresponds to the surface coverage of the surfactant at cmc. The structural properties of the adsorbed monolayer, such as the number density profiles of different components normal to the plane of the interface (i.e., along the *z* direction) and the thickness of the monolayer (d_h, d_t), are calculated. It is observed that significant roughness developed at the interface during the time scale of the simulation with extensive mixing of the head and tail segments of the surfactant chains. The calculated thickness of the adsorbed layer has been found to agree reasonably well with experimental results.[14,33] It is found that there is a significant fraction of the surfactants with their headgroups reoriented within the aqueous layer close to the interface. This occurs due to strong interaction between the long polar headgroups of the surfactants and the interfacial water molecules. Such unique orientational behavior was observed earlier for this class of surfactants with smaller headgroups, namely, $C_{12}E_2$.[20] Such a strong interaction with water is also reflected in slower reorientational motion of the surfactant headgroups. We observed significant anomaly in the diffusion behavior of the surfactant molecules within the time scale of the simulation.

The dynamics of the interfacial water molecules are also investigated in detail. Both translational and reorientational motions of the water molecules have been found to be restricted near the interface. An important observation from this study has been the drastic increase in both translational and rotational motion of water molecules with a small increase in distance from the surfactant headgroups. We noticed that the average relaxation time for the reorientational motion of water in different regions of the aqueous layer can drastically vary with distance from the surfactant headgroups.

It is important to obtain a further microscopic level understanding of the interaction between the surfactants and the interfacial water molecules. In particular, it would be interesting to study the formation and breaking of hydrogen bonds and their lifetimes between the water molecules and the surfactant headgroups. This will help obtaining a greater molecular level understanding of the properties of surfactant monolayers adsorbed at an interface. Some of these aspects are presently under investigation in our laboratory.

Acknowledgment. This work was supported in part by generous grants from the Council of Scientific and Industrial Research (CSIR) and the Department of Science and Technology (DST), Government of India. One of us (J.C.) thanks Sudip Chakraborty for many useful discussions.

References

(1) Laughlin, R. G. *The Aqueous Phase Behavior of Surfactants*; Academic Press: New York, 1994.

(2) Funari, S. S.; Rapp, G. *J. Phys. Chem. B* **1997**, *101*, 732−739.

(3) Briganti, G.; Segre, A. L.; Capitani, D.; Casieri, C.; Mesa, C. L. *J. Phys. Chem. B* **1999**, *103*, 825−830.

(4) Capitani, D.; Casieri, C.; Briganti, G.; Mesa, C. L.; Segre, A. L. *J. Phys. Chem. B* **1999**, *103*, 6088−6095.

(5) Gragson, D. E.; McCarty, B. M.; Richmond, G. L. *J. Phys. Chem.* **1996**, *100*, 14272−14275.

(6) Conboy, J. C.; Messmer, M. C.; Richmond, G. L. *J. Phys. Chem. B* **1997**, *101*, 6724−6733.

(7) Conboy, J. C.; Messmer, M. C.; Richmond, G. L. *Langmuir* **1998**, *14*, 6722−6727.

(8) Grubb, S. G.; Kim, M. W.; Raising, T.; Shen, Y. R. *Langmuir* **1988**, *4*, 452−454.

(9) Zhang, Z. H.; Tsuyumoto, I.; Kitamori, T.; Sawada, T. *J. Phys. Chem. B* **1998**, *102*, 10284−10287.

(10) Piasecki, D. A.; Wirth, M. J. *J. Phys. Chem.* **1993**, *97*, 7700−7705.

(11) Tian, Y.; Umemura, J.; Takenaka, T.; Kunitake, T. *Langmuir* **1988**, *4*, 1064−1066.

(12) Kjellin, U. R. M.; Claesson, P. M.; Linse, P. *Langmuir* **2002**, *18*, 6745−6753.

(13) Lu, J. R.; Li, Z. X.; Thomas, R. K.; Staples, E. J.; Thompson, L.; Tucker, I.; Penfold, J. *J. Phys. Chem.* **1994**, *98*, 6559−6567.

(14) Lu, J. R.; Su, T. J.; Li, Z. X.; Thomas, R. K.; Staples, E. J.; Tucker, I.; Penfold, J. *J. Phys. Chem. B* **1997**, *101*, 10332−10339.

(15) Penfold, J.; Staples, E. J.; Tucker, I.; Thomas, R. K. *J. Colloid Interface Sci.* **1998**, *201*, 223−232.

(16) Lu, J. R.; Li, Z. X.; Thomas, R. K.; Binks, B. P.; Crichton, D.; Fletcher, P. D. I.; McNab, J. R.; Penfold, J. *J. Phys. Chem. B* **1998**, *102*, 5785−5793.

(17) Penfold, J.; Thomas, R. K. *Phys. Chem. Chem. Phys.* **2002**, *4*, 2648−2652.

(18) Tarek, M.; Tobias, D. J.; Klein, M. L. *J. Phys. Chem.* **1995**, *99*, 1393−1402.

(19) Schweighofer, K. J.; Essmann, U.; Berkowitz, M. *J. Phys. Chem. B* **1997**, *101*, 3793−3799.

(20) Bandyopadhyay, S.; Chanda, J. *Langmuir* **2003**, *19*, 10443−10448.

(21) Chanda, J.; Chakraborty, S.; Bandyopadhyay, S. *J. Phys. Chem. B* **2005**, *109*, 471−479.

(22) Wijmans, C. M.; Linse, P. *J. Phys. Chem.* **1996**, *100*, 12583−12591.

(23) Schweighofer, K. J.; Essmann, U.; Berkowitz, M. *J. Phys. Chem. B* **1997**, *101*, 10775−10780.

(24) Dominguez, H.; Berkowitz, M. L. *J. Phys. Chem. B* **2000**, *104*, 5302−5308.

(25) Kuhn, H.; Rehage, H. *J. Phys. Chem. B* **1999**, *103*, 8493−8501.

(26) Kuhn, H.; Rehage, H. *Phys. Chem. Chem. Phys.* **2000**, *2*, 1023−1028.

(27) Kuhn, H.; Rehage, H. *Colloid Polym. Sci.* **2000**, *278*, 114−118.

(28) da Rocha, S. R. P.; Johnston, K. P.; Rossky, P. J. *J. Phys. Chem. B* **2002**, *106*, 13250−13261.

(29) Stone, M. T.; da Rocha, S. R. P.; Rossky, P. J.; Johnston, K. P. *J. Phys. Chem. B* **2003**, *107*, 10185−10192.

(30) Rekvig, L.; Hafskjold, B.; Smit, B. *J. Chem. Phys.* **2004**, *120*, 4897−4905.

(31) Rekvig, L.; Hafskjold, B.; Smit, B. *Phys. Rev. Lett.* **2004**, *92*, 116101.

(32) Dominguez, H. *J. Phys. Chem. B* **2002**, *106*, 5915−5924.

(33) Lu, J. R.; Li, Z. X.; Thomas, R. K.; Staples, E. J.; Tucker, I.; Penfold, J. *J. Phys. Chem.* **1993**, *97*, 8012−8020.

(34) Martyna, G. J.; Tuckerman, M. E.; Tobias, D. J.; Klein, M. L. *Mol. Phys.* **1996**, *87*, 1117−1157.

(35) Tuckerman, M. E.; Yarne, D. A.; Samuelson, S. O.; Hughs, A. L.; Martyna, G. J. *Comput. Phys. Commun.* **2000**, *128*, 333−376.

(36) Darden, T.; York, D.; Pedersen, L. *J. Chem. Phys.* **1993**, *98*, 10089−10092.

(37) Procacci, P.; Darden, T.; Marchi, M. *J. Phys. Chem.* **1996**, *100*, 10464−10468.

(38) Procacci, P.; Marchi, M.; Martyna, G. J. *J. Chem. Phys.* **1998**, *108*, 8799−8803.

(39) Allen, M. P.; Tildesley, D. J. *Computer Simulation of Liquids;* Clarendon: Oxford, 1987.

(40) Berendsen, H. J. C.; Grigera, J. R.; Straatsma, T. P. *J. Phys. Chem.* **1987**, *91*, 6269−6271.

(41) Martin, M. G.; Siepmann, J. I. *J. Phys. Chem. B* **1998**, *102*, 2569−2577.

(42) Jorgensen, W. L. *J. Phys. Chem.* **1986**, *90*, 1276−1284.

(43) Briggs, J. M.; Matsui, T.; Jorgensen, W. L. *J. Comput. Chem.* **1990**, *11*, 958−971.

(44) Tu, K.; Tobias, D. J.; Blasie, J. K.; Klein, M. L. *Biophys. J.* **1996**,*70*, 595−608.

(45) Liu, P.; Harder, E.; Berne, B. J. *J. Phys. Chem. B* **2004**, *108*, 6595−6602.

(46) Christensen, M.; Pedersen, J. B. *J. Chem. Phys.* **2003**, *119*, 5171−5175.

(47) Balasubramanian, S.; Bagchi, B. *J. Phys. Chem. B* **2002**, *106*, 3668−3672.

(48) Balasubramanian, S.; Pal, S.; Bagchi, B. *Phys. Rev. Lett.* **2002**, *89*, 115505.

(49) Faeder, J.; Ladanyi, B. M. *J. Phys. Chem. B* **2000**, *104*, 1033−1046.

(50) Bandyopadhyay, S.; Chakraborty, S.; Balasubramanian, S.; Pal, S.; Bagchi, B. *J. Phys. Chem. B* **2004**, *108*, 12608−12616.

CT050019Y